

## Long-term evolution and gravitational wave radiation of neutron stars with differential rotation induced by $r$ -modes \*

Yun-Wei Yu, Xiao-Feng Cao and Xiao-Ping Zheng

Institute of Astrophysics, Huazhong Normal University, Wuhan 430079, China;  
[yuyw@phy.ccnu.edu.cn](mailto:yuyw@phy.ccnu.edu.cn)

Received 2008 November 7; accepted 2009 June 26

**Abstract** In a second-order  $r$ -mode theory, Sá and Tomé found that the  $r$ -mode oscillation in neutron stars (NSs) could induce stellar differential rotation, which naturally leads to a saturated state of the oscillation. Based on a consideration of the coupling of the  $r$ -modes and the stellar spin and thermal evolution, we carefully investigate the influences of the differential rotation on the long-term evolution of isolated NSs and NSs in low-mass X-ray binaries, where the viscous damping of the  $r$ -modes and its resultant effects are taken into account. The numerical results show that, for both kinds of NSs, the differential rotation can significantly prolong the duration of the  $r$ -modes. As a result, the stars can keep nearly a constant temperature and constant angular velocity for over a thousand years. Moreover, the persistent radiation of a quasi-monochromatic gravitational wave would also be predicted due to the long-term steady  $r$ -mode oscillation and stellar rotation. This increases the detectability of gravitational waves from both young isolated and old accreting NSs.

**Key words:** stars: neutron — stars: evolution — stars: rotation — gravitational waves

### 1 INTRODUCTION

$R$ -modes in a perfectly fluid star with arbitrary rotation arise due to the action of the Coriolis force with positive feedback (Andersson 1998; Friedman & Morsink 1998), succumbing to gravitational radiation-driven Chandrasekhar-Friedman-Schutz instability (Chandrasekhar 1970; Friedman & Schutz 1978). In contrast, the growth of the modes can be suppressed by the viscosity of the stellar matter. Thus, the  $r$ -mode evolution is determined by the competition between the viscous damping effect and the destabilizing effect due to gravitational radiation. Based on the law of angular momentum conservation, a phenomenological model describing the  $r$ -mode evolution was proposed by Owen et al. (1998) and improved by Ho & Lai (2000). However, although the suppression of the oscillation by viscosities was considered there, an unbounded growth of the modes would still have resulted since the model does not include nonlinear effects. In order to avoid this problem, an artificial saturated  $r$ -mode amplitude is usually put into the model by hand. Then, the spin and thermal evolution and gravitational wave radiation of neutron stars (NSs) suffering from  $r$ -mode instability can be calculated (e.g., Owen et al. 1998; Levin 1999; Ho & Lai 2000; Watts & Andersson 2002; Heyl 2002).

To understand  $r$ -modes more deeply and judge their astrophysical implications, it is necessary to take into account some nonlinear effects that could naturally give rise to a saturated  $r$ -mode amplitude (e.g., Schenk et al. 2002; Arras et al. 2003; Brink et al. 2004a,b, 2005). As an important nonlinear

---

\* Supported by the National Natural Science Foundation of China.

effect, differential rotation induced by  $r$ -modes was first studied by Rezzolla et al. (2000, 2001), who analytically used linearized fluid equations by expanding the velocity of a fluid element located at a certain point in powers of the mode amplitude, averaging over a gyration, and retaining only the lowest-order nonvanishing term. Soon afterwards, some numerical studies (Stergioulas & Font 2001; Lindblom et al. 2001) confirmed the existence of such drifts. More exactly, Sá (2004) solved the fluid equations within a nonlinear theory up to second order in the mode amplitude and described the stellar differential rotation analytically. By extending Owen et al.'s model to this nonlinear case, Sá & Tomé (2005, 2006) further obtained a saturated amplitude of the  $r$ -modes self-consistently. Their study also investigated the early (millions of seconds after the birth) spin evolution of nascent NSs under the influence of the differential rotation, but did not cover the phase during which the viscous damping effect becomes important. In this paper, we would find that the long-term spin and thermal evolution of isolated NSs and NSs in low-mass X-ray binaries (LMXBs) can also be remarkably influenced by the differential rotation by prolonging the duration of the  $r$ -modes. Moreover, in view of the prolonged  $r$ -modes, gravitational waves could be expected to be continuously emitted from both young isolated and old accreting NSs.

In the next section, we briefly review the second-order  $r$ -mode theory of Sá (2004). Then, we exhibit the coupling thermal,  $r$ -mode, and spin evolution equations in Section 3, where some typical numerical solutions are given for both isolated and accreting NSs. In Section 4, we estimate the detectability of gravitational waves from NSs. Finally, a summary is given in Section 5.

## 2 THE SECOND-ORDER $R$ -MODES

For a rotating barotropic Newtonian star, the  $r$ -mode solutions of perturbed fluid equations can be found in spherical coordinates  $(r, \theta, \phi)$  to first order in  $\alpha$  as (Lindblom et al. 1998),

$$\delta^{(1)}v^r = 0, \quad (1)$$

$$\delta^{(1)}v^\theta = \alpha\Omega C_l l \left(\frac{r}{R}\right)^{l-1} \sin^{l-1}\theta \sin(l\phi + \omega t), \quad (2)$$

$$\delta^{(1)}v^\phi = \alpha\Omega C_l l \left(\frac{r}{R}\right)^{l-1} \sin^{l-2}\theta \cos\theta \cos(l\phi + \omega t), \quad (3)$$

and to second order in  $\alpha$  as (Sá 2004)

$$\delta^{(2)}v^r = \delta^{(2)}v^\theta = 0, \quad (4)$$

$$\begin{aligned} \delta^{(2)}v^\phi = & \frac{1}{2}\alpha^2\Omega C_l^2 l^2 (l^2 - 1) \left(\frac{r}{R}\right)^{2l-2} \sin^{2l-4}\theta \\ & + \alpha^2\Omega A r^{N-1} \sin^{N-1}\theta, \end{aligned} \quad (5)$$

where  $\alpha$  represents the amplitude of the oscillation,  $R$  and  $\Omega$  are the radius and angular velocity of the unperturbed star,  $\omega = -\Omega(l+2)(l-1)/(l+1)$ ,  $C_l = (2l-1)!!\sqrt{(2l+1)}/[2\pi(2l)!(l+1)]$ , and  $A$  and  $N$  are two constants determined by the initial condition. For simplicity, Sá & Tomé (2005) suggested  $N = 2l - 1$  and redefined  $A$  by introducing a new free parameter  $K$  as  $A = \frac{1}{2}K C_l^2 l^2 (l+1)R^{2-2l}$ . For the most unstable  $l = 2$   $r$ -mode of primary interest to us, the second-order solution  $\delta^{(2)}v^\phi$  shows a differential rotation of the star induced by the  $r$ -mode oscillation, i.e., large scale drifts of fluid elements along stellar latitudes. Using  $\delta^{(1)}v^i$  and  $\delta^{(2)}v^i$ , the corresponding Lagrangian displacements  $\xi^{(1)i}$  and  $\xi^{(2)i}$  can be derived and then the physical angular momentum of the  $l = 2$   $r$ -mode can be calculated up to second order in  $\alpha$  as (Sá 2004; Sá & Tomé 2005)

$$J_r = J^{(1)} + J^{(2)} = \frac{(4K + 5)}{2}\alpha^2 \tilde{J} M R^2 \Omega, \quad (6)$$

where  $\tilde{J} = 1.635 \times 10^{-2}$  and

$$J^{(1)} = - \int \rho \partial_\phi \xi^{(1)i} \left( \partial_t \xi_i^{(1)} + v^k \nabla_k \xi_i^{(1)} \right) dV, \quad (7)$$

$$J^{(2)} = \frac{1}{\Omega} \int \rho v^i \left[ \partial_t \xi^{(1)k} \nabla_i \xi_k^{(1)} + v^k \nabla_k \xi^{(1)m} \nabla_i \xi_m^{(1)} + \partial_t \xi_i^{(2)} + v^k \left( \nabla_i \xi_k^{(2)} + \nabla_k \xi_i^{(2)} \right) \right] dV. \quad (8)$$

Meanwhile, following Owen et al. (1998) and Sá (2004), we further express the energy of the  $l = 2$   $r$ -mode by

$$E_r = J^{(2)}\Omega - \frac{1}{3}J^{(1)}\Omega = \frac{(4K+9)}{2}\alpha^2 \tilde{J}MR^2\Omega^2. \quad (9)$$

When  $K = -2$ ,  $J^{(2)}$  vanishes and the expressions of  $J_r$  and  $E_r$  return to their canonical forms (Owen et al. 1998), in other words, the differential rotation disappears. Both the physical angular momentum and energy of the  $r$ -mode are increased by gravitational radiation back reaction and decreased by viscous damping, which yields

$$\frac{dJ_r}{dt} = \frac{2J_r}{\tau_g} - \frac{2J_r}{\tau_v}, \quad (10)$$

$$\frac{dE_r}{dt} = \frac{2E_r}{\tau_g} - \frac{2E_r}{\tau_v}, \quad (11)$$

where  $\tau_g = 3.26\tilde{\Omega}^{-6}$  s,  $\tau_{sv} = 2.52 \times 10^8 T_9^2$  s, and  $\tau_{bv} = 6.99 \times 10^8 T_9^{-6} \tilde{\Omega}^{-2}$  s are the timescales of the gravitational radiation, shear viscous damping, and bulk viscous damping (for  $l = 2$ ), respectively (Owen et al. 1998), and  $\tau_v = (\tau_{sv}^{-1} + \tau_{bv}^{-1})^{-1}$ . Hereafter, the convention  $Q_x \equiv Q/10^x$  and  $\tilde{\Omega} \equiv \Omega/\sqrt{\pi G \bar{\rho}}$  are adopted in cgs units. These timescales are obtained with a polytropic equation of state as  $p = k\rho^2$  for NSs, with  $k$  chosen so that the mass and radius of the star are  $M = 1.4 M_\odot$  and  $R = 12.53$  km. The competition between the gravitational destabilizing effect that is dependent on  $\Omega$  and the  $T$ -dependent viscous damping effect determines an instability window in the  $T - \Omega$  plane, where a small perturbation would grow exponentially due to  $(\tau_g^{-1} - \tau_v^{-1})^{-1} > 0$ .

### 3 EVOLUTION OF NSS

#### 3.1 Thermal Evolution Equation

Considering the temperature dependence of the viscosities, we would like to show the thermal evolution equation of a NS first before calculating the  $r$ -mode evolution, which reads as (Shapiro & Teuklosky 1983; Yakovlev et al. 1999; Yakovlev & Pethick 2004)

$$\frac{dT}{dt} = -\frac{1}{C_v}(L_\nu + L_\gamma - H_{sv}), \quad (12)$$

where  $C_v \approx 10^{39} T_9$  erg K<sup>-1</sup> is the heat capacity of the star. On one hand, the NS can be cooled by neutrino and photon energy release, the luminosities of which are estimated to be  $L_\nu \approx 10^{40} T_9^8$  erg s<sup>-1</sup> (for the modified URCA process) and  $L_\gamma = 4\pi R^2 \sigma T_s^4 \approx 10^{35} T_9^{2.2}$  erg s<sup>-1</sup>, respectively. For the black-body luminosity  $L_\gamma$ , we use the relationship  $T_s \approx 3.34 \times 10^6 T_9^{0.55}$  between the interior ( $T$ ) and surface ( $T_s$ ) temperatures (Gudmundsson et al. 1983). Specifically, the temperature dependence of  $L_\nu$  and  $L_\gamma$  indicates that the cooling of the NS at high ( $> 10^8$  K) and low ( $< 10^8$  K) temperatures would be dominated by neutrino and photon emissions, respectively. On the other hand, the shear viscous dissipation of the  $r$ -mode can gradually convert a part of the oscillation energy into heat energy. Using the shear viscous damping timescale, we estimate the rate of this energy conversion as

$$H_{sv} = \frac{2E_r}{\tau_{sv}} = 2.0 \times 10^{43} (4K+9) \alpha^2 T_9^{-2} \tilde{\Omega}^2 \text{ erg s}^{-1}. \quad (13)$$

During the very early ages of a nascent NS, during which the above heating effect is much weaker than the neutrino cooling effect, an approximative temperature evolution can be solved from Equation (12) as  $T = T_i(1+t/t_c)^{-1/6}$ , where  $T_i$  is the initial temperature and  $t_c \approx (20/T_{i,10}^6)$  s. However, as the  $r$ -mode increases, the cooling of the star would be effectively resisted by the heating effect, as demonstrated by some previous studies (e.g., Zheng et al. 2006).

### 3.2 Isolated NSs

A simple phenomenological model for the  $r$ -mode evolution was proposed by Owen et al. (1998) first and further improved by Ho & Lai (2000) based on a consideration of angular momentum conservation. For a normal NS with a strong magnetic field ( $\sim 10^{10} - 10^{13}$  G), besides the braking effect due to gravitational radiation, the spindown of the star resulting from magnetic dipole radiation should also be taken into account. So, we write the decrease of the total angular momentum of the star as (Owen et al. 1998; Ho & Lai 2000; Sá & Tomé 2005)

$$\frac{dJ}{dt} = -\frac{3\alpha^2 \tilde{J} M R^2 \Omega}{\tau_g} - \frac{I \Omega}{\tau_m}, \quad (14)$$

where  $\tau_m = 1.35 \times 10^9 B_{12}^{-2} (\Omega / \sqrt{\pi G \bar{\rho}})^{-2}$  s is the magnetic braking timescale and  $I = \tilde{I} M R^2$  with  $\tilde{I} = 0.261$  is the moment of inertia of the star. Due to the  $r$ -mode oscillation, the total angular momentum of the star could be separated into two parts, i.e.,  $J = I \Omega + J_r$ . Then, Equations (10) and (14) yield

$$\frac{d\alpha}{dt} = \left[ 1 + \frac{4}{3}(K+2)Q\alpha^2 \right] \frac{\alpha}{\tau_g} - \left[ 1 + \frac{1}{3}(4K+5)Q\alpha^2 \right] \frac{\alpha}{\tau_v} + \frac{\alpha}{2\tau_m}, \quad (15)$$

$$\frac{d\Omega}{dt} = -\frac{8}{3}(K+2)Q\alpha^2 \frac{\Omega}{\tau_g} + \frac{2}{3}(4K+5)Q\alpha^2 \frac{\Omega}{\tau_v} - \frac{\Omega}{\tau_m}, \quad (16)$$

where  $Q = 3\tilde{J}/2\tilde{I} = 0.094$ . During the very early ages of nascent NSs when  $\tau_g \ll (\tau_v, \tau_m)$ , the viscous and magnetic terms in the above two equations can be omitted. Combining this simplification with the analytical temperature  $T = T_i(1 + t/t_c)^{-1/6}$ , Sá & Tomé (2005, 2006) obtained an analytical solution of Equations (15) and (16) for  $t < 0.3$  yr. For convenience, their analytical solution can also be expressed by two asymptotic functions as follows (Sá & Tomé 2006):

$$\alpha(t) \approx \begin{cases} \alpha_i \exp(t/\tau_{g,i}), & \text{for } t < t_a \\ \frac{3.56}{\sqrt{K+2}} (t/\tau_{g,i})^{1/10}, & \text{for } t > t_a \end{cases} \quad (17)$$

$$\Omega(t) \approx \begin{cases} \Omega_i \left[ 1 - \frac{4}{3}(K+2)Q\alpha_i^2 \exp(2t/\tau_{g,i}) \right], & \text{for } t < t_a \\ 0.63 (t/\tau_{g,i})^{-1/5}, & \text{for } t > t_a \end{cases} \quad (18)$$

where  $\alpha_i$  and  $\Omega_i$  are the initial  $r$ -mode amplitude and angular velocity, respectively, and  $\tau_{g,i} = 3.26\tilde{\Omega}_i^{-6}$  s. The transition time  $t_a \approx [521 - 18.5 \ln(K+2)]$  s is determined by the condition  $d^2\alpha/dt^2 = 0$  and corresponds to the amplitude  $\alpha(t_a) = [12(K+2)Q]^{-1/2}$  (Sá & Tomé 2006).

As the temperature and angular velocity decrease, the viscous damping timescale would become comparable to the gravitational radiation timescale. Therefore, it is necessary to completely solve the coupling Equations (12), (15), and (16) in order to depict the long-term history of NSs. For different values of  $K$  ( $\geq -5/4$ ), we show some numerical evolution curves of the  $r$ -mode amplitude in Figure 1. As indicated by the thin solid lines, the two increasing segments of the evolution curves can be fitted by Equation (17) well, i.e., the amplitude first increases exponentially and then gradually reaches a saturation value. About one tenth of a year later after the birth of the stars, the growth of the  $r$ -mode would be stopped and instead, the amplitude nearly stays constant until an extremely fast decay due to  $(\tau_g^{-1} - \tau_v^{-1})^{-1} < 0$ . The higher the value of  $K$  is, the longer the duration of this plateau phase is.

In order to exhibit the influence of the differential rotation on the  $r$ -mode evolution, for an example, we plot the  $r$ -mode evolution curves for  $K = 100$  (differential rotation case) and  $-2$  (non-differential rotation case) in Figure 2(a). As mentioned above, the non-differential rotation model ( $K = -2$ ) is incapable of determining a saturation amplitude. So, for comparison, we put an effective saturation amplitude in the case of  $K = -2$  by hand, which is taken to equal the one calculated from the differential rotation case (e.g.,  $\alpha_{\text{sat}} = 1.1$  for  $K = 100$ ). Correspondingly, Figures 2(b) and 2(c) show the temporal evolution of the stellar angular velocity and temperature, respectively, for both  $K = 100$  and  $-2$ . For a differential-rotation NS, we can divide its evolution during the  $r$ -mode oscillation into six phases

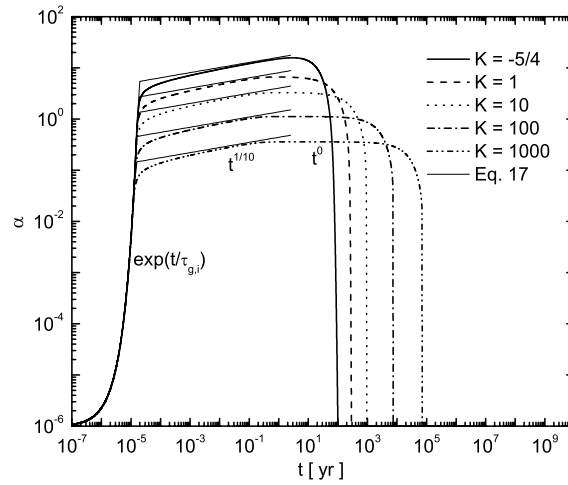


**Fig. 1** Evolution of the  $r$ -mode amplitude of an isolated NS with a magnetic field  $B = 10^{12}$  G for different values of  $K$  (thick lines). For a comparison, the thin solid lines are given by the asymptotic functions shown in Eq. (17). The initial values of the  $r$ -mode amplitude, angular velocity, and temperature are taken to be  $\alpha_i = 10^{-6}$ ,  $\Omega_i = \Omega_K \equiv \frac{2}{3}\sqrt{\pi G \bar{\rho}}$ , and  $T_i = 10^{10}$  K, respectively, where  $\Omega_K$  is the Keplerian angular velocity at which the star starts shedding mass at the equator.

**Table 1** Different phases of evolution of a young isolated differential-rotation NS, during which  $\alpha$ ,  $\Omega$ , and  $T$  have different temporal behaviors as listed below. The coefficient  $a = \frac{4}{3}(K + 2)Q\alpha_i^2$ .

Phases	I	II	IIIa	IIIb	IV	V
$\alpha(t) \propto$	$\exp(t/\tau_{g,i})$	$\exp(t/\tau_{g,i})$	$t^{1/10}$	$t^{1/10}$	$t^0$	decrease
$\Omega(t) \propto$	$t^0$	$1 - a \exp(2t/\tau_{g,i})$	$t^{-1/5}$	$t^{-1/5}$	$t^0$	increase
$T(t) \propto$	$t^{-1/6}$	$t^{-1/6}$	$t^{-1/6}$	$t^0$	$t^0$	decrease

(denoted by I-V), the temporal behaviors of which are listed in Table 1. In particular, within phase IV, the extremely slow variation in  $\Omega$  and  $T$  makes the timescales  $\tau_g$  and  $\tau_v$  nearly constant. Thus, the contemporaneous  $r$ -mode oscillation can remain steady for a long period.

Comparing the differential with non-differential rotation cases, we can find that: (1) The differential rotation obviously strengthens the gravitational braking effect for  $t < 0.3$  yr (phases II and III). However, subsequently, from one tenth to a few thousand years (phases IV and V), the spindown of the star due to gravitational radiation would be effectively held back by an angular momentum transfer from  $J_r$  to  $I\Omega$ , although during this time, the  $r$ -mode always stays in the saturated state. Due to the existence of this angular velocity plateau (i.e.,  $d\Omega/dt \sim 0$ ; phase IV), a quasi-monochromatic gravitational wave can be expected to be persistently emitted from a young ( $< 10^3$  yr) NS (see Sect. 4). (2) The obvious difference in the temperature plateaus between the cooling curves with  $K = 100$  and  $-2$  indicates that the heating effect due to  $r$ -mode dissipation is also strengthened dramatically by the differential rotation. As a result, the NS with differential rotation can keep a high constant temperature for a few thousand years. Finally, we show the evolution trajectories of isolated NSs for  $K = 100$  and  $-2$  in the  $T - \Omega$  plane in Figure 3, where the six evolution phases for the differential-rotation star are labeled with their durations. The point marked by a solid circle represents phase IV, at which the star would stay for a thousand years. From this figure, we can clearly see that the differential-rotation star can accelerate its rotation without any external cause (e.g., accretion) within phase V. In other words, the star would experience a self-acceleration phase.

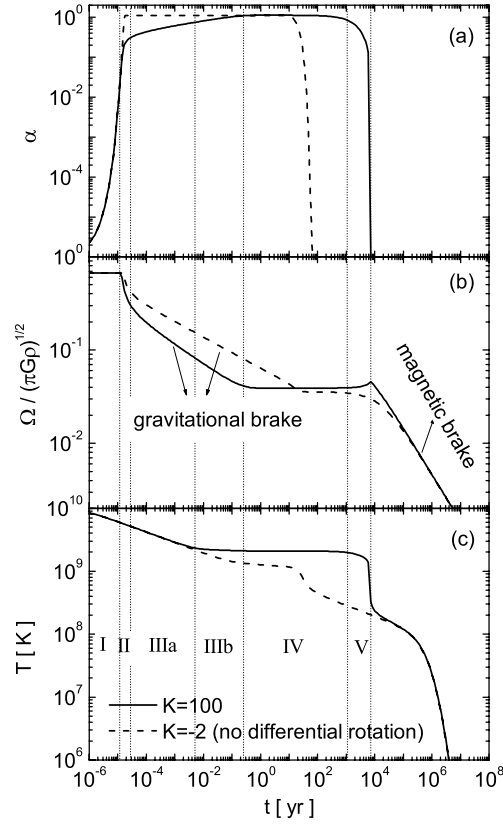


**Fig. 2** Evolutionary curves of  $\alpha$ ,  $\Omega$ , and  $T$  of an isolated NS with a magnetic field  $B = 10^{12}$  G for  $K = 100$  (solid lines; differential rotation case) and  $K = -2$  (dashed lines; non-differential rotation case). The initial conditions are the same as those in Fig. 1. For the differential-rotation star, its evolution can be divided into several phases (denoted by I-V) by the vertical dotted lines, and the temporal behaviors of  $\alpha$ ,  $\Omega$ , and  $T$  during these phases are listed in Table 1.

To summarize, during the early part of the  $r$ -mode evolution (phases I, II, and III), the rotation energy of the star ( $\frac{1}{2}I\Omega^2$ ) is converted into oscillation energy, internal energy, and the energy of gravitational waves. In contrast, during the later parts (phases IV and V), the energy deposited in the  $r$ -mode would be released gradually via heating the star and accelerating the stellar rotation due to viscosity.

### 3.3 NSs in LMXBs

For NSs in LMXBs, whose magnetic fields are usually found to be relatively weak ( $\sim 10^8 - 10^9$  G), their angular velocity could be increased by accreting materials from their companion star. Then, the evolution of the stellar angular momentum would be determined by the competition between the gravitational radiation and accretion as (Levin 1999; Zhang & Dai 2008)

$$\frac{dJ}{dt} = -\frac{3\alpha^2 \tilde{J} M R^2 \Omega}{\tau_g} + \dot{M} R^2 \Omega_K, \quad (19)$$

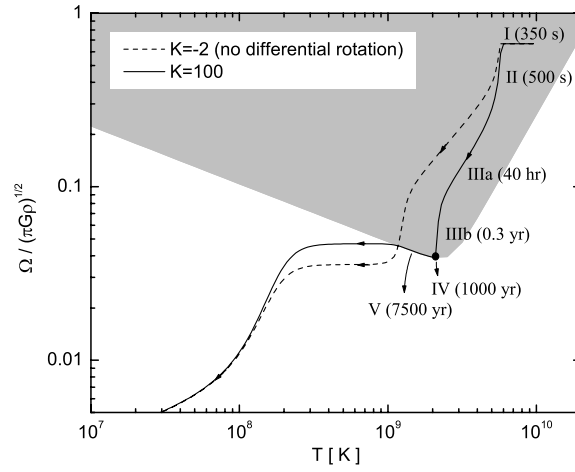


**Fig. 3** Evolutionary trajectories of an isolated NS with  $B = 10^{12}$  G in the  $T - \Omega$  plane for  $K = 100$  (solid line; differential rotation case) and  $K = -2$  (dashed line; non-differential rotation case). The initial conditions are the same as those in Fig. 1. The shaded region exhibits the  $r$ -mode instability window. For the differential-rotation star, its evolution phases are labeled by their durations in the brackets.

where  $\dot{M}$  is the accretion rate and the velocity of the accretion disk is assumed to be equal to the Keplerian velocity  $\Omega_K$ . Combining Equations (10) and (19), we can get

$$\frac{d\alpha}{dt} = \left[ 1 + \frac{4}{3}(K+2)Q\alpha^2 \right] \frac{\alpha}{\tau_g} - \left[ 1 + \frac{1}{3}(4K+5)Q\alpha^2 \right] \frac{\alpha}{\tau_v} - \frac{1}{\bar{I}} \frac{\Omega_K}{\Omega} \frac{\alpha}{2\tau_a}, \quad (20)$$

$$\frac{d\Omega}{dt} = -\frac{8}{3}(K+2)Q\alpha^2 \frac{\Omega}{\tau_g} + \frac{2}{3}(4K+5)Q\alpha^2 \frac{\Omega}{\tau_v} + \left( \frac{1}{\bar{I}} \frac{\Omega_K}{\Omega} - 1 \right) \frac{\Omega}{\tau_a}, \quad (21)$$

where  $\tau_a = M/\dot{M}$  is defined as an accretion timescale.

We plot the evolutionary trajectories of accreting NSs in the  $T - \Omega$  plane for  $K = 100$  and  $-2$  in Figure 4. Different from the case of the isolated NSs shown in Figure 3, the spin-up by accretion can be more effective than the spin-down by magnetic dipole radiation for the accreting stars during their old age ( $\sim 10^5 - 10^6$  yr). In particular, if the accretion rate is high enough, cyclic evolution could be found (black lines). This is qualitatively consistent with the results in Levin (1999) and Heyl (2002). However, for  $\dot{M} = 10^{-8} M_\odot \text{ yr}^{-1}$  specifically, we do not obtain the cycle as Levin (1999) did. There are two reasons for this difference: (1) In the calculations of Levin (1999), an effective shear viscous damping timescale  $\tau_{sv} = 1.03 \times 10^6 T_g^2 \text{ s}$  was taken by hand in order to fit the observational data, whereas we adopt a theoretical value of  $\tau_{sv} = 2.52 \times 10^8 T_g^2 \text{ s}$  from Owen et al. (1998); (2) The cooling effect due to thermal radiation, which can effectively pull the star away from the  $r$ -mode instability window in the  $T - \Omega$  plane, was ignored in Levin (1999).

The temporal behaviors of  $\alpha$ ,  $\Omega$ , and  $T$  within one cycle are exhibited in Figure 5. In order to show the detailed features of the cycle clearly, the time-axes in the left- and right-hand panels of Figure 5 are drawn on normal and logarithmic scales, respectively. To be specific, the left-hand panel shows that the period of the cyclic evolution is mildly shortened by the differential rotation ( $4.5 \times 10^5$  yr vs.  $5.6 \times 10^5$  yr), and the right-hand panel indicates that the duration of the  $r$ -mode oscillation within one cycle is prolonged significantly (3900 yr vs. 65 yr). Similar to the early evolution of young isolated NSs shown in Figure 2, the evolution during the  $r$ -mode oscillation within one cycle of the old ( $> 10^5$  yr) accreting NSs can be divided into five phases. A comparison between Figures 2 and 5 shows that: (1) during phases I' and II', the spin-down of accreting NSs is very similar to that of isolated NSs during phases I and II, but the thermal evolution of the two kinds of NSs are completely contrary to each

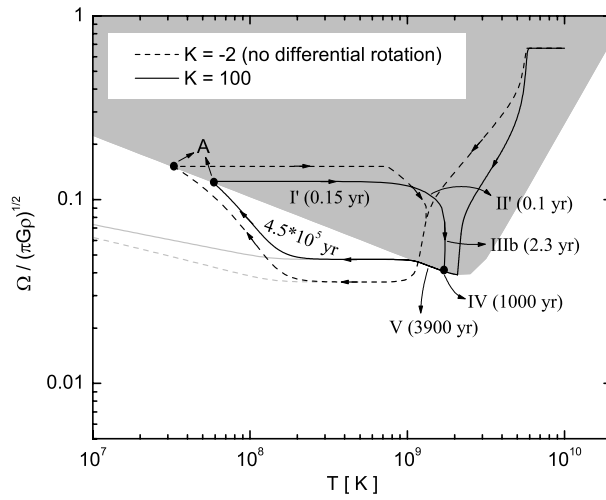


**Fig. 4** The same as Fig. 3 but for a NS with  $B = 10^8$  G in a LMXB. The black and grey lines correspond to the accretion rates  $\dot{M} = 10^{-7} M_{\odot} \text{ yr}^{-1}$  and  $10^{-8} M_{\odot} \text{ yr}^{-1}$ , respectively.

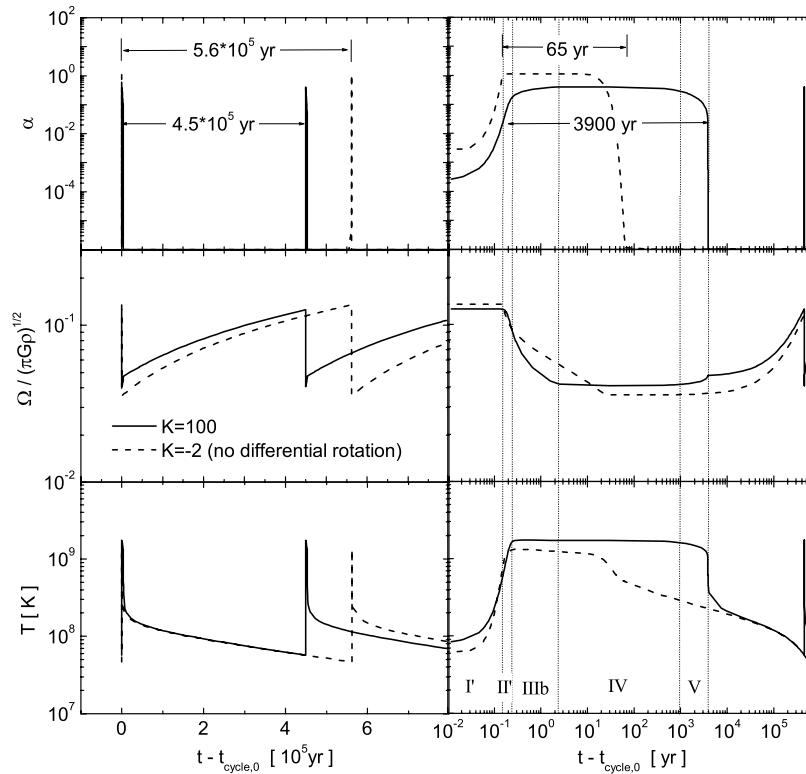


**Fig. 5** Evolutionary curves of  $\alpha$ ,  $\Omega$ , and  $T$  during the cyclic evolution of a NS with  $B = 10^8$  G in a LMXB for  $K = 100$  (solid lines; differential rotation case) and  $K = -2$  (dashed lines; non-differential rotation case). The beginning of the cycle is set at point A that is marked in Fig. 4, and the age of the star at point A is denoted by  $t_{\text{cycle},0}$ .

other during these phases. (2) the temporal behaviors of young isolated and old accreting NSs during phases IIIb, IV, and V seem to be nearly identical except for the durations of the specific phases. This indicates that the young isolated and old accreting NSs may be able to produce some of the same astrophysical phenomena, e.g., self-acceleration and monochromatic gravitational wave radiation (see the next section).

#### 4 DETECTABILITY OF GRAVITATIONAL WAVES

Using the obtained  $r$ -mode amplitude and angular velocity, we can estimate the amplitude of the emitted gravitational waves as follows (Owen et al. 1998; Sá & Tomé 2006):

$$|h(t)| = 1.3 \times 10^{-24} \alpha(t) \left[ \frac{\Omega(t)}{\Omega_K} \right]^3 \left( \frac{20 \text{ Mpc}}{d_L} \right), \quad (22)$$

where  $d_L$  is the distance to the star. Then, the frequency-domain gravitational wave amplitude (i.e., the Fourier transform of  $h(t)$ ,  $\tilde{h}(f) = \int_{-\infty}^{\infty} e^{2\pi i f t} h(t) dt$ ) can be calculated by (Owen et al. 1998; Sá & Tomé 2006)

$$|\tilde{h}(f)| = \frac{|h(t)|}{\sqrt{df/dt}}, \quad (23)$$

where  $f = 2\Omega/(3\pi)$  is the frequency of the gravitational waves for the  $l = 2$  mode. From the above two equations, we know that NSs with a relatively large  $r$ -mode amplitude and a nearly invariable angular velocity (e.g., NSs during phases IV and I'<sup>1</sup>) may be able to produce monochromatic gravitational radiation with a relatively high value of  $|\tilde{h}(f)|$ . In order to analyze the possibility of detecting gravitational waves with the laser interferometer detectors LIGO and Virgo, in Figure 6, we compare the characteristic amplitude of the signal,  $h_c(f) = f|\tilde{h}(f)|$ , with the rms strain noise in the detectors,  $h_{\text{rms}}(f) = \sqrt{f S_h(f)}$ , for both isolated (left-hand panel) and accreting (right-hand panel) NSs. For the noise spectral density of the detectors,  $S_h(f)$ , some approximative expressions can be found in Sá & Tomé (2006) for LIGO, Virgo, and advanced LIGO.

On one hand, as found by Sá & Tomé (2006), the spike of  $h_c(f)$  at  $f_{\text{max}} = 2\Omega_K/(3\pi)$  that was predicted by Owen et al. (1998; see the thick dashed lines in Fig. 6) disappears under the influence of the differential rotation, and the numerical results of  $h_c(f)$  for  $f > 100$  Hz in Figure 6 can be perfectly fitted by the following analytical expression

$$h_c(f) = \frac{5.5 \times 10^{-22}}{\sqrt{K+2}} \sqrt{\frac{f}{f_{\text{max}}}} \left( \frac{20 \text{ Mpc}}{d_L} \right). \quad (24)$$

On the other hand, surprisingly, a new remarkable spike emerges within the range of  $\sim 60 - 90$  Hz, where the approximative analysis in Sá & Tomé (2006) is inapplicable. From Figures 2 and 5, we know that the angular velocity of the NSs is nearly invariable and thus  $|df/dt| \rightarrow 0$  during phase IV, while the  $r$ -mode stays in the saturated state all the time. As a result, both young isolated and old accreting NSs could emit quasi-monochromatic ( $\sim 70$  Hz) gravitational waves for several hundred years. Similarly, due to the existence of Phase I', another weaker spike at  $\sim 220$  Hz would also be predicted for accreting NSs, which is shown in the right-hand panel of Figure 6.

Using matched filtering, the power signal-to-noise ratio  $(S/N)^2$  of a detection from  $t_0$  to  $t_{\text{det}}$  is given by (Owen et al. 1998; Sá & Tomé 2006)

$$\left( \frac{S}{N} \right)^2 = 2 \int_{t_0}^{t_{\text{det}}} \left[ \frac{f(t)h(t)}{h_{\text{rms}}(f(t))} \right]^2 dt, \quad (25)$$

<sup>1</sup> During both phases IV and I', the braking and accelerating effects cancel each other and thus the NSs can have a steady rotation.

where  $t_0$  is the beginning of the observation. In Table 2, we list some values of S/N with different  $t_{\text{det}}$  and  $K$  for an isolated NS by setting  $t_0$  at the birth of the star.

Since the spike of  $h_c(f)$  within  $\sim 60 - 90$  Hz would appear about 0.3 yr after the increase of the  $r$ -mode, the signal-to-noise ratio obtained from a long-term detection could be much higher than that from a short-period detection (i.e., the case focused on in Sá & Tomé 2006).

**Table 2** Signal-to-noise ratios of gravitational wave detections for different detectors, different values of  $K$ , and different detection durations for an isolated NS at  $d_L = 20$  Mpc. The beginning of the detection is set at the birth of the star.

$t_{\text{det}} - t_0$	LIGO			Virgo			Advanced LIGO		
	$K = 1$	10	100	1	10	100	1	10	100
0.3 yr	0.65	0.33	0.11	0.51	0.26	0.01	9.18	4.62	1.59
1 yr	0.67	0.34	0.12	0.54	0.27	0.01	9.63	4.90	1.69
10 yr	0.81	0.44	0.15	0.77	0.42	0.15	13.53	7.46	2.63
30 yr	0.91	0.55	0.20	1.06	0.62	0.22	18.60	10.98	3.93

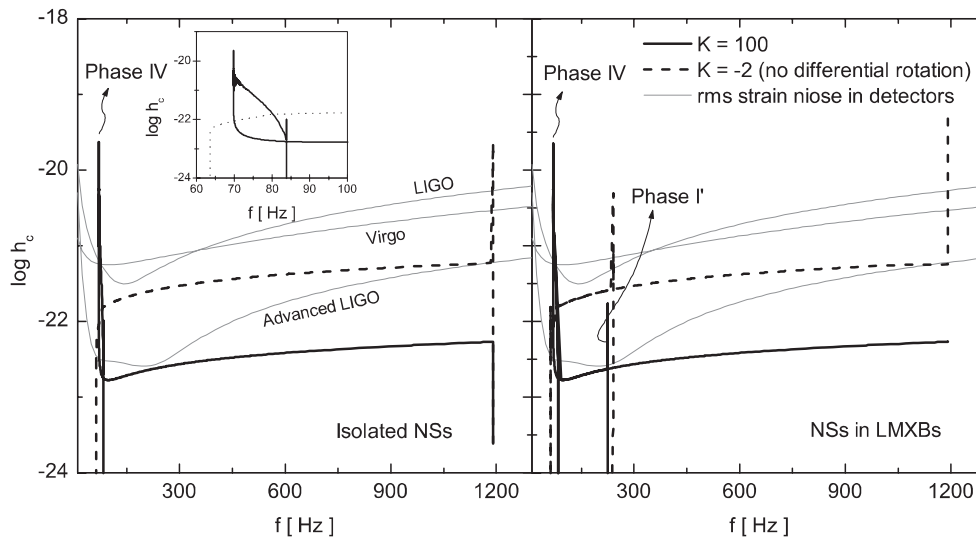


**Fig. 6** A comparison of the characteristic amplitudes of gravitational waves (*thick lines*) with the rms strain noise in the detectors (*thin dotted lines*). The details of the curves of  $h_c(f)$  within  $\sim 60 - 90$  Hz are shown in the insert panel, where solid and dashed lines correspond to  $K = 100$  and  $K = -2$ , respectively.

## 5 SUMMARY

A second-order  $r$ -mode theory was developed by Sá (2004) and Sá & Tomé (2005). This theory predicts that the  $r$ -mode oscillation could naturally induce differential rotation in neutron stars, which can determine a saturation amplitude of the  $r$ -mode. In the framework of this theory, we investigate the long-term spin and thermal evolution of isolated NSs and NSs in LMXBs. In our calculations, the effects of heating due to  $r$ -mode dissipation, gravitational and magnetic braking, and accretion are taken into account. Our results show that, to a certain extent, the linear  $r$ -mode evolutionary model using an artificial saturation amplitude can describe the basic features of the evolution of NSs qualitatively,

but predicts an obviously underestimated  $r$ -mode duration. By considering the differential rotation, we may obtain a slight self-acceleration and an enhanced temperature plateau for NSs. In particular, due to an effective transfer of angular momentum from  $J_r$  to  $I\Omega$ , the spindown of NSs can be stopped for a few hundred years, whereas the gravitational radiation still exists during this period. As a result, long-lasting quasi-monochromatic gravitational wave radiation is predicted, which increases the detectability of gravitational waves from both young ( $< 10^3$  yr) isolated and old ( $> 10^5$  yr) accreting NSs.

**Acknowledgements** This work is supported by the National Natural Science Foundation of China (Grant Nos. 10603002 and 10773004). Yu Y. W. is also supported by the Scientific Innovation Foundation of Huazhong Normal University.

## References

- Andersson, N. 1998, ApJ, 502, 708  
Arras, P., Flanagan, E. E., Morsink, S. M., et al. 2003, ApJ, 591, 1129  
Brink, J., Teukolsky, S. A., & Wasserman, I. 2004a, Phys. Rev. D, 70, 121501  
Brink, J., Teukolsky, S. A., & Wasserman, I. 2004b, Phys. Rev. D, 70, 124017  
Brink, J., Teukolsky, S. A., & Wasserman, I. 2005, Phys. Rev. D, 71, 064029  
Chandrasekhar, S. 1970, Phys. Rev. Lett., 24, 611  
Friedman, J. L., & Morsink, S. M. 1998, ApJ, 502, 714  
Friedman, J. L., & Schutz, B. F. 1978, ApJ, 221, 937  
Gudmundsson, E. H., Pethick, C. J., & Epstein, R. I. 1983, ApJ, 272, 286  
Heyl, J. S. 2002, ApJ, 574, L57  
Ho, W. C. G., & Lai, D. 2000, ApJ, 543, 386  
Levin, Y. 1999, ApJ, 517, 328  
Lindblom, L., Owen, B. J., & Morsink, S. M. 1998, Phys. Rev. Lett., 80, 4843  
Lindblom, L., Tohline, J. E., & Vallisneri, M. 2001, Phys. Rev. Lett., 86, 1152  
Owen, B. J., Lindblom, L., Cutler, C., Schutz, B. F., Vecchio, A., & Andersson, N. 1998, Phys. Rev. D, 58, 084020  
Rezzolla, L., Lamb, F. K., & Shapiro, S. L. 2000, ApJ, 531, L139  
Rezzolla, L., Lamb, F. K., Frederick, K., Markovic, D., & Shapiro, S. L. 2001, Phys. Rev. D, 64, 104013  
Sá, P. M. 2004, Phys. Rev. D, 69, 084001  
Sá, P. M., & Tomé, B. 2005, Phys. Rev. D, 71, 044007  
Sá, P. M., & Tomé, B. 2006, Phys. Rev. D, 74, 044011  
Schenk, A. K., Arras, P., Flanagan, E. E., Teukolsky, S. A., & Wasserman, I. 2002, Phys. Rev. D, 65, 024001  
Shapiro, S. L., & Teukolsky, S. A. 1983, Black holes, white dwarfs and neutron stars (New York: Wiley)  
Stergioulas, N., & Font, J. A. 2001, Phys. Rev. Lett., 86, 1148  
Watts, A. L., & Andersson, N. 2002, MNRAS, 333, 943  
Yakovlev, D. G., Levenfish, K. P., & Shibano, Yu. A. 1999, Phys. Usp., 42, 737 [arXiv: astro-ph/9906456]  
Yakovlev, D. G., & Pethick, C. J. 2004, ARA&A, 42, 169  
Zhang, D., & Dai, Z. G. 2008, ApJ, 683, 329  
Zheng, X. P., Yu, Y. W., & Li, J. R. 2006, MNRAS, 369, 376